Korean J. Chem. Eng., 35(2), 503-510 (2018)
DOI: 10.1007/s11814-017-0297-5

pISSN: 0256-1115
eISSN: 1975-7220

Effects of torrefaction on physical properties, chemical composition and reactivity of microalgae

Neeranuch Phusunti*,†, Worasak Phetwarotai, and Surajit Tekasakul***

*Department of Chemistry, Faculty of Science, Prince of Songkla University, Hat Yai, Songkhla 90112, Thailand
**Department of Materials Science and Technology, Faculty of Science, Prince of Songkla University, Hat Yai, Songkhla 90112, Thailand
(*Received 10 April 2017 • accepted 18 October 2017*)

Abstract−Torrefaction of the microalga *Chlorella vulgaris* was carried out in a fixed-bed tubular reactor under various conditions of temperature (150-300 °C), time (15-60 min), and atmosphere (inert or oxidative). The impact of torrefaction and its various conditions on the mass yield, physical properties, chemical composition, and reactivity of the microalgal biomass was assessed and compared with those of the raw material. After torrefaction, the morphology, proximate analysis, ultimate analysis, higher heating value analysis, chemical compositions, and thermal behavior of the biomass were carried out. The results show that torrefaction temperature influenced mass yield and changes in the microalgae's properties more than torrefaction time and atmosphere. Torrefaction at 200 °C, for 30 min in an inert atmosphere led to the highest calorific value of torrefied microalgae. In addition, torrefaction reduced the thermal degradation rates of the remaining protein and carbohydrate fractions in the biomass, but accelerated the degradation rate of the lipids fraction.

Keywords: Torrefaction, *Chlorella vulgaris*, Microalgae, Mass Yield, Reactivity

INTRODUCTION

Due to the depletion of fossil fuels and concerns about environmental problems, biomass is becoming more recognized as an important source of renewable fuels and valuable chemicals. Sources of biomass vary around the world. Wood, agricultural waste, industrial waste, energy crops and aquatic plants are all useful resources depending on their availability from area to area. Although several thermochemical conversion processes are available to convert biomass into different forms of energy and chemicals, there are some unavoidable disadvantages of biomass that need to be overcome. Heterogeneity, uneven physical properties, low energy density, high moisture content and its hygroscopic nature limit the use of raw biomass in bioenergy production and they also impact efficient and economic handling, storage, transportation, and conversion technologies [1-3]. To enhance the utilization of biomass conversion for certain products, some biomass resources have to be pre-treated before they can be used as a solid fuel.

In recent years, interest in the use of torrefaction to improve the properties of biomass has grown. Thermal treatment of biomass by torrefaction is considered at relatively mild temperatures around 200-300 °C under an inert or oxidative atmosphere [4]. Nitrogen is the most commonly used medium for non-oxidative torrefaction, while oxygen-containing carrier gases are used in oxidative torrefaction to produce mainly solid residues or solid fuel [5,6]. Different atmospheres can lead to different levels of solid yield from biomass torrefaction [7]. In addition, treatment by torrefaction can improve the properties of biomass as a solid fuel. Several reports have shown that torrefied biomass can have higher energy density, better hydrophobic properties, less microbial degradation, and improved grindability [8-10]. Torrefied biomass is considered more suitable for long term storage and transportation [11], and improvements to the conversion of biomass include a faster rate of combustion, cleaner process, and higher quality products [12,13]. The torrefied biomass can be used as solid fuel for co-firing with coal at power plants [14]. Produced as pellets and briquettes, it is suitable for gasification and pyrolysis processes with enhanced product properties [15,16]. The improvements to the qualities of biomass brought about by torrefaction are attributed to the thermal degradation of the components of the biomass, so that the constituent structures and functional groups change permanently [17].

Over the past several years, the torrefaction of lignocellulosic biomass like wood, grass and agricultural biomass has been extensively studied, and substantial research has taken place into the torrefaction of high moisture biomass, such as food waste [18], sewage sludge [19], and aquatic plants [20,21]. But, despite these initiatives, few studies have been reported on the torrefaction of algal biomass, whether macroalgae or microalgae. The advantages of algal biomass over terrestrial biomass are its rapid growth, high productivity, non-competition with food markets, and lower water requirement. These benefits support its extensive use in renewable energy production, and the cost of drying algal biomass has been reduced [21], leading to more interest. However, torrefaction behavior is very complicated and may vary because of the diversity of the physical and chemical properties of the raw materials [22,23]. Lignocellulosic biomass consists of hemicelluloses, cellulose, and lignin. Moisture and most of the hemicelluloses can be removed during torrefaction in the form of water, organic acids, lightweight com-

†To whom correspondence should be addressed.
E-mail: neeranuch.p@psu.ac.th

pounds and incondensable gases [24]. However, three main biochemical constituents of microalgae--proteins, carbohydrates, and lipids--exhibit thermal decomposition characteristics distinct from the lignocellulosic biomass. Thus, the effects of torrefaction on microalgae are implicitly different from those on lignocellulosic biomass and are also influenced by the torrefaction conditions such as temperature, reaction time, atmosphere, and the apparatus used [25-27].

In this work, the torrefaction of *Chlorella vulgaris* microalgae was conducted in a fixed-bed tubular reactor. Torrefaction factors of temperature (150-300 °C), time (15-60 min), and atmosphere (inert and oxidative) were studied. The impact of torrefaction and its various conditions was studied and the mass yield, physical properties, chemical composition, and reactivity of the torrefied microalgal biomass were compared with those of the raw material.

EXPERIMENTAL SECTION

1. Materials

Green microalgae, *Chlorella vulgaris*, were from Sunrise Nutrachem Group Co., Limited (Qingdao, China). The moisture content of the dried microalgae, as received, was 5.5%. Their particle size was in the range of 0.791-493.6 μm in diameter. The microalgae biomass was stored at 4 °C in a sealed container until use. The fundamental properties of the samples were analyzed, and the results are shown in Table 1.

2. Torrefaction Experiment

The torrefaction experiments on the *Chlorella vulgaris* biomass were conducted in a fixed bed tubular reactor with an electrical furnace. Torrefaction was performed at 150 °C, 200 °C, 250 °C, and 300°C, and the process times in the study were 15, 30, 45, and 60 min. Also, the atmosphere of torrefaction was investigated under inert and oxidative conditions by flowing nitrogen gas and compressed air at 400 mL/min, respectively. The carrier gas flow was kept constant throughout the torrefaction experiment to remove the volatiles from the reactor tube. In each experiment, microalgal biomass with a total mass of 10 g (±5%) was placed in the reaction tube and heated to reach the set torrefaction temperature. Then, the sample was torrefied for a given time period. After treatment, the solid product was cooled and weighed to determine the solid yield. It was then placed in an airtight container and stored in a desiccator for further analysis. Each experiment was repeated three times under the same conditions, and the results were found to be reproducible.

Table 1. The proximate analysis, ultimate analysis, main components and high heating value of *Chlorella vulgaris* used in this study

Proximate analysis (wt%)	
Moisture content	5.47
Volatile matter	71.38
Fixed carbon	16.07
Ash	7.08
Ultimate analysis (wt%)	
C	45.66
H	5.90
O[a]	31.95
N	9.05
S	0.36
Main components (wt%)	
Proteins	31.17
Carbohydrates	22.70
Lipids	13.99
HHV (MJ/kg)	18.77

[a]By difference

3. Characterization Methods

Listed in Table 1 are the proximate, ultimate and main components of the raw biomass, in the form of lipids, carbohydrates, and protein, and its higher heating value (HHV). The proximate analysis of the biomass was performed by thermogravimetric analyzer, TGA7 (Perkin Elmer, USA). A microalgal powder sample (10 mg) was heated from 50 °C to 110 °C in a nitrogen atmosphere with a flow rate at 20 mL/min and kept at 110 °C for 5 min. Then the sample was heated to 900 °C at a rate of 10 °C/min. After that the atmosphere was replaced with oxygen gas and combusted for 20 min. The ultimate analysis was carried out using a CHNS-O Analyzer, Flash 1112 EA Series EA, Thermoquest. The oxygen content was calculated by difference after determining the content of C, H, N, and S. The main chemical components of the microalgae were measured. Briefly, the crude protein content was determined by TCA-acetone extraction following the method of Lowry et al. [28]. A standard aqueous solution of Bovine serum albumin, BSA (0-500 μg) was used for the preparation of the calibration curve. The carbohydrate content was determined by the phenol-sulfuric acid method [29], using glucose solutions as the standard substance. Crude lipids were extracted from the microalgal samples using a modification of the Bligh and Dyer method with 2 : 1 v/v methanol : chloroform [30]. The main components was determined in three duplicates to determine the reproducibility. The high heating value (HHV) was calculated by the following equation [31].

$$HHV\ (kJ/kg)=3.55C^2-232C-2230H+51.2C\times H+131N+20{,}600 \quad (1)$$

The thermal behavior of raw samples and torrefied materials was ascertained by non-isothermal thermogravimetric analysis (TGA). In each TGA experiment, 10 mg samples were analyzed via thermogravimetric analyzer, TGA7 (Perkin Elmer, USA). Using a heating rate of 10 °C/min, the sample was heated from 50 °C to 600 °C under a nitrogen flow rate of 20 mL/min to prevent an oxidative atmosphere. The micrographs were produced using a scanning electron microscope (Quanta400, FEI, Czech Republic). The FTIR spectra of dried raw and torrefied microalgae were obtained using Fourier transform infrared spectrometer, FTIR (Spectrum BX, Perkin Elmer) at room temperature. The dried sample was mixed with potassium bromide (KBr) powder and pressed into pellets before analysis.

RESULTS AND DISCUSSION

1. Torrefaction Yield

The mass yield of biomass torrefied at various temperatures,

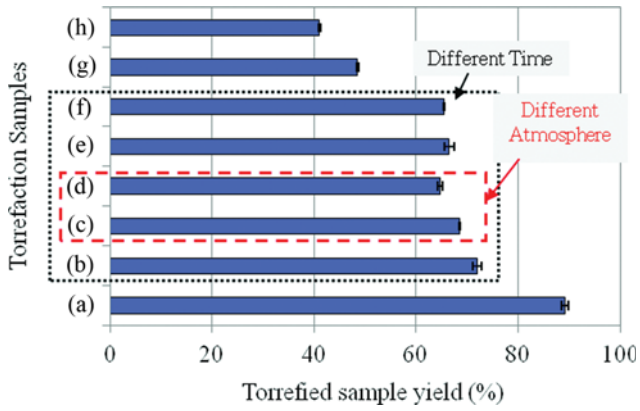

Fig. 1. Effect of torrefaction temperature, time, and atmosphere on the torrefied materials ((a) 150 °C, 30 min, inert; (b) 200 °C, 15 min, inert; (c) 200 °C, 30 min, inert; (d) 200 °C, 30 min, oxidative; (e) 200 °C, 45 min, inert; (f) 200 °C, 60 min, inert; (g) 250 °C, 30 min, inert; (h) 300 °C, 30 min, inert).

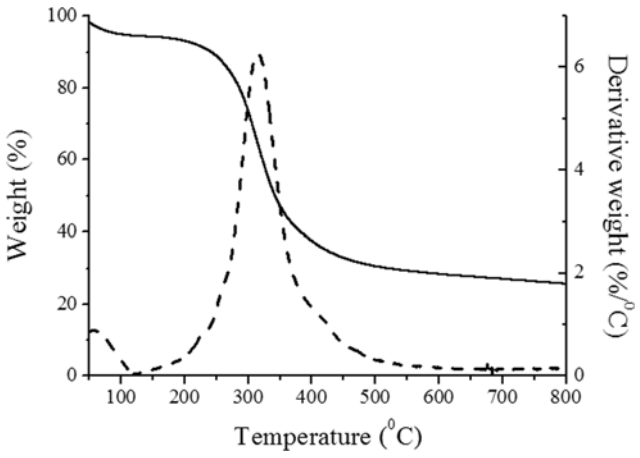

Fig. 2. TGA and DTG curves for microalgae at 10 °C/min in nitrogen atmosphere.

times and atmospheres is presented in Fig. 1. The yield decreased with an increase in torrefaction temperature. The results are in agreement with Wu and coworkers [20]. Torrefied at 150 °C (Fig. 1(a)), the mass yield of the biomass was about 90 wt%, while at 250 °C (Fig. 1(g)) and 300 °C (Fig. 1(h)) the mass yield was lower than 50 wt%. The influence of temperature on the mass yield was similar to the case of lignocellulosic biomass [32]. On the other hand, in comparison to temperature, the torrefaction time produced only a slightly significant effect. It can be seen that mass yield decreased quickly from 150 °C to 300 °C at the same torrefaction time, but at 200 °C it was between 71.94-65.42 wt% with varying times of 15-60 min (Fig. 1(b), (c), (e), (f)), indicating that the influence of torrefaction temperature on mass yield is more significant than torrefaction time. Similar finding has also been reported for the wood torrefaction [33]. For atmosphere effect, the oxidative atmosphere (Fig. 1(d)) led to a lower yield of torrefied biomass than the inert atmosphere (Fig. 1(c)). Similar results were also obtained in the torrefaction of lignocellulosic biomass due to the oxidation of all the biomass components [7,34]. For a microalgal biomass, the mass loss is attributed to the decomposition of the highly reactive fractions of proteins and carbohydrates [35].

The TGA and derivative thermogravimetric (DTG) curves for the microalgae are shown in Fig. 2. There were three stages in their

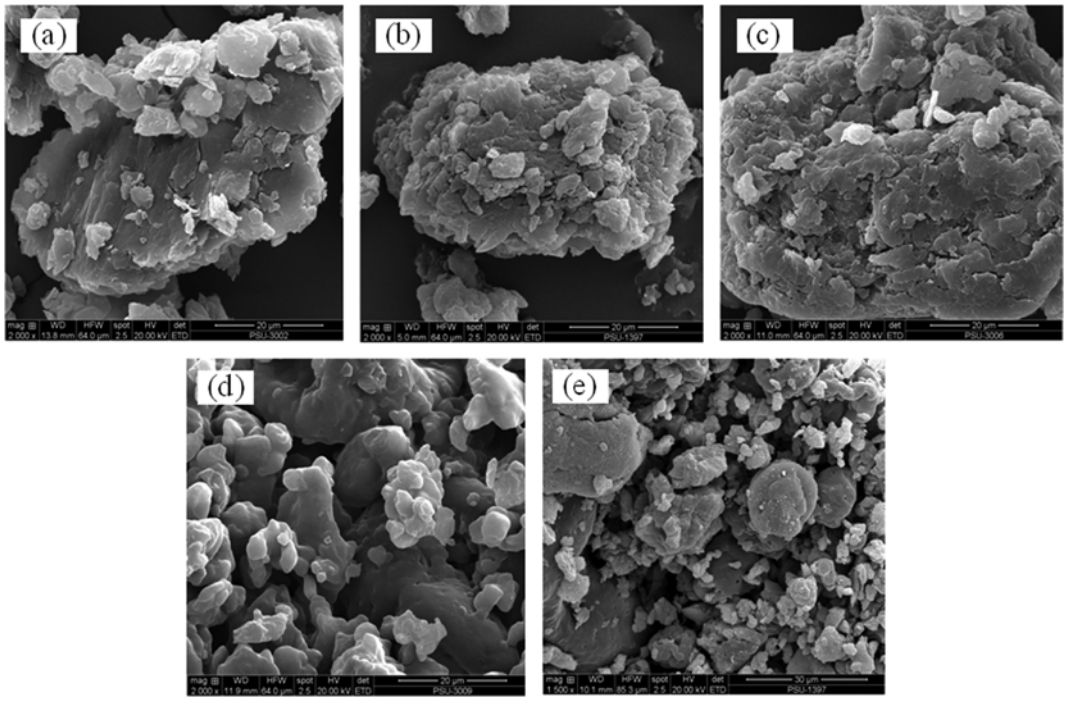

Fig. 3. SEM images of (a) raw and torrefied microalgal biomass at (b) 150 °C, (c) 200 °C, (d) 250 °C, and (e) 300 °C with magnification of 2000x.

pyrolysis. The first stage was the removal of moisture and light volatiles below 120 °C. The second was the main devolatilization at 120-500 °C with a large amount of generated volatiles. The maximum weight loss for microalgae happened at 315 °C, which was attributed mainly to protein and carbohydrate fractions [35,36]. Torrefaction temperatures below these maximum weight loss points were chosen for this work. The weight loss in the thermogravimetric data was consistent with the mass yield of torrefied microalgae with regard to the torrefaction time. The third stage appeared after 500 °C. At this stage, carbonaceous matter gradually decomposed.

2. Effect of Torrefaction Temperature on Morphology of Raw and Torrefied Microalgae

Scanning electron microscopy (SEM) was used to investigate the morphology of the raw and torrefied microalgal biomass. Fig. 3(a)-(e) shows the SEM photographs of the raw and torrefied materials at different torrefaction temperatures with 2000x magnification. There are no pores visible on the surface of both raw and torrefied materials at 150 °C and 200 °C, while the surface of materials torrefied at 250 °C and 300 °C appear rougher. At 150 °C and 200 °C, compared with the raw biomass surface, more cracks occurred as the temperature increased and the materials became fragmented. The presence of cracks was also observed at torrefaction of lignocellulosic biomass [37]. In Fig. 3(d) of material torrefied at 250 °C, various small particles can be observed on the surface with cavities, and these features become more obvious and the size of particles smaller in material torrefied at 300 °C in Fig. 3(e). The higher the torrefaction temperature, the more the composition is degraded, and therefore the hollower the structure of the torrefied microalgae becomes. The compact structure became looser and was broken into small particles.

3. Effect of Torrefaction on Chemical Compositions

The results of the ultimate analysis and ash content at different torrefaction temperatures compared with the raw material are shown in Fig. 4(a). Fig. 4(b) presents the ultimate analysis and ash content at different torrefaction times. It is observed that the O and H content in the torrefied biomass decreased with increasing temperature and slightly decreased with increasing torrefaction time. On the other hand, the carbon content increased with increasing temperature and time, due to the carbonization of the microalgae during the torrefaction process. Those trends are in agreement with the torrefaction of lignocellulosic biomass [8,11] and macroalgae [21]. The nitrogen and sulfur content of the raw material were 9.05 wt% and 0.36 wt% respectively, and these values slightly increased to 11.51 and to 0.76, in samples torrefied at 300 °C. The

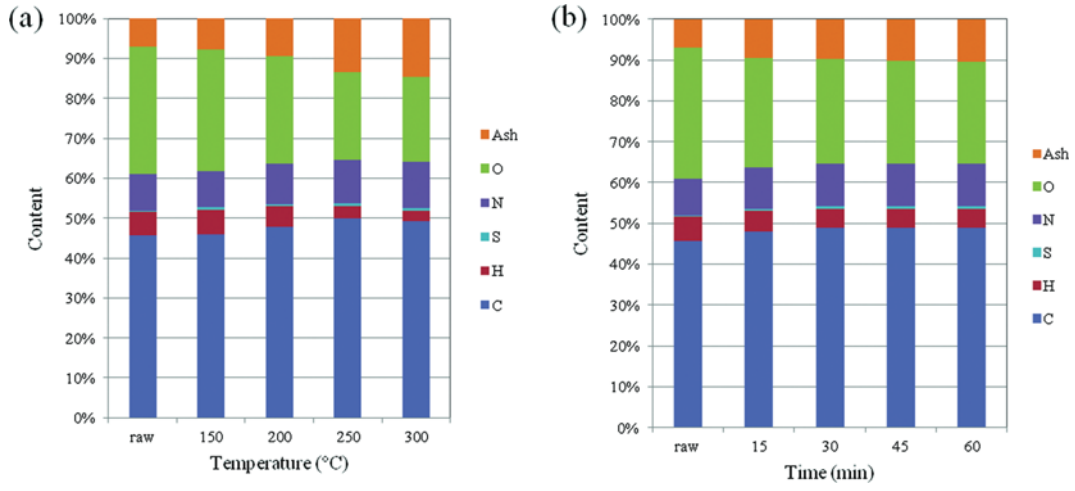

Fig. 4. Ultimate analysis and ash content of raw and torrefied microalgae at different (a) torrefaction temperatures and (b) torrefaction times.

Table 2. Proximate analysis and calorific values of raw and torrefied microalgae

Torrefaction conditions			Proximate analysis (wt%, dry basis)				HHV (MJ/kg)*
Temperature (°C)	Time (min)	Atmosphere	Moisture	VM	FC	Ash	
Raw material	-	-	5.47	71.38	16.07	7.08	18.77
150	30	N_2	3.69	72.73	15.90	7.68	19.04
200	15	N_2	3.08	65.64	21.77	9.51	19.30
	30	N_2	2.34	61.02	26.88	9.75	19.48
	30	O_2	2.46	60.41	26.78	10.35	18.98
	45	N_2	3.52	59.02	27.31	10.15	19.42
	60	N_2	3.55	57.49	28.64	10.33	19.40
250	30	N_2	4.36	41.57	40.76	13.31	18.71
300	30	N_2	5.83	38.97	40.49	14.71	18.14

*Calculated from ultimate analysis data [31]

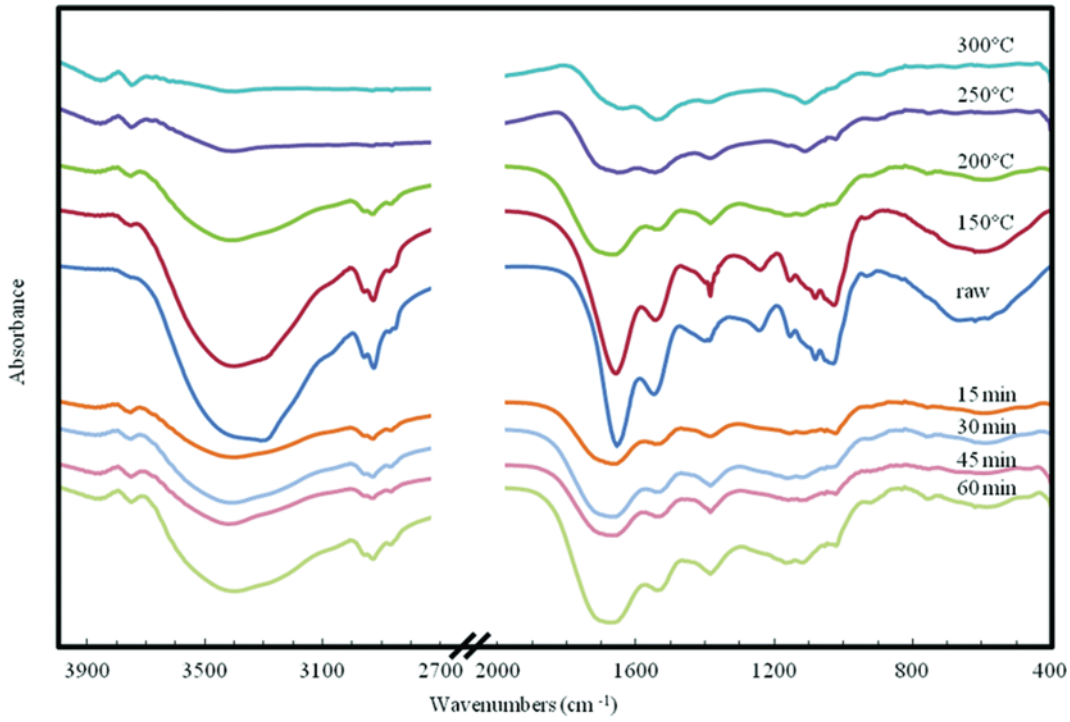

Fig. 5. FTIR spectra of raw and torrefied biomass.

ash content of the same samples increased because the inorganic matter stayed in the solid phase during the process [21].

The results of proximate and calorific analyses under different torrefaction conditions are shown in Table 2: The moisture content of the sample slightly decreased from raw up to 200 °C and then increased to 300 °C to finish with a moisture content a little higher than that of the raw material. In addition, the moisture content of the torrefied microalgae was lower than that of the raw material at every torrefaction time. The volatile matter shows a significant reduction with increasing temperature and time, but fixed carbon produced the opposite result. These contrasting results are attributed to mass loss during torrefaction, because volatile matter is combustible, but fixed carbon is not lost at those torrefaction temperatures. The high heating value (HHV) of the raw material was 18.77 MJ/kg. Once the microalgae underwent torrefaction at 150 °C and 200 °C, the HHV increased. However, with torrefaction temperatures of 250 °C and 300 °C, the HHV decreased to 18.71 and 18.14 MJ/kg, respectively. For different torrefaction times at 200 °C, all the torrefied material had higher HHV than that of raw material. In addition, the product had a higher HHV when torrefied under an inert atmosphere than under an oxidative atmosphere. Lu et al. [7] reported the decrease in HHV of oil palm fiber with an increase in temperature under air atmosphere, but under nitrogen atmosphere, its HHV increased with the increase of temperature. The change of HHV under different torrefaction conditions can be affected by the changed composition content in materials. A high carbon content led to a high calorific value, but the presence of moisture and ash lowers the calorific value, which reflects the quality of the torrefied biomass as a solid fuel for combustion. Furthermore, volatile matter and fixed carbon contribute to heating value, and the low ratio of volatile matter to the fixed carbon of these torrefied microalgae indicates a better quality fuel, which generates less smoke during combustion [20].

Fig. 5 presents the FTIR spectra of the raw materials and microalgae torrefied at different temperatures and times. Some important structures can be indicated in FTIR spectrum of raw microalgae in terms of the main biochemical compositions (proteins, carbohydrates, and lipids). First, the protein structure is indicated by the Amide I band for -C=O stretching around 1,654 cm^{-1}, the Amide II band for -NH vibration around 1,548 cm^{-1}, and the Amide III band around 1,244 cm^{-1}, which overlapped with P=O bond vibration in nucleic acids [38]. Second, carbohydrates are indicated by the vibration of -CO of the aliphatic groups around 1,028 cm^{-1}. Third, the presence of lipids is shown around 2,928 cm^{-1} by the band of aliphatic chains due to the symmetrical and asymmetrical stretching of -CH_2- groups and by the bands between 3,000 and 3,050 cm^{-1} for the vibration of -CH linked to unsaturated C-C bonds [39]. Another wide band between 3,300 and 3,400 cm^{-1} is assigned to -OH stretching of carbohydrates, proteins, and lipids.

On comparing the intensity of the bands in each region of the spectra for the raw microalgal biomass and torrefied biomass, a decrease in intensity of several bands was clearly observed for at various torrefaction temperatures. The same comparison does not reveal significant changes when different torrefaction times are considered. These results support the influence of temperature rather than time on the decomposition of reactive fractions in the torrefaction of microalgal biomass.

4. Effect of Torrefaction on Reactivity of Torrefied Microalgae

The thermogravimetric analysis (TGA) and derivative thermogravimetric (DTG) analysis of the raw and torrefied microalgae

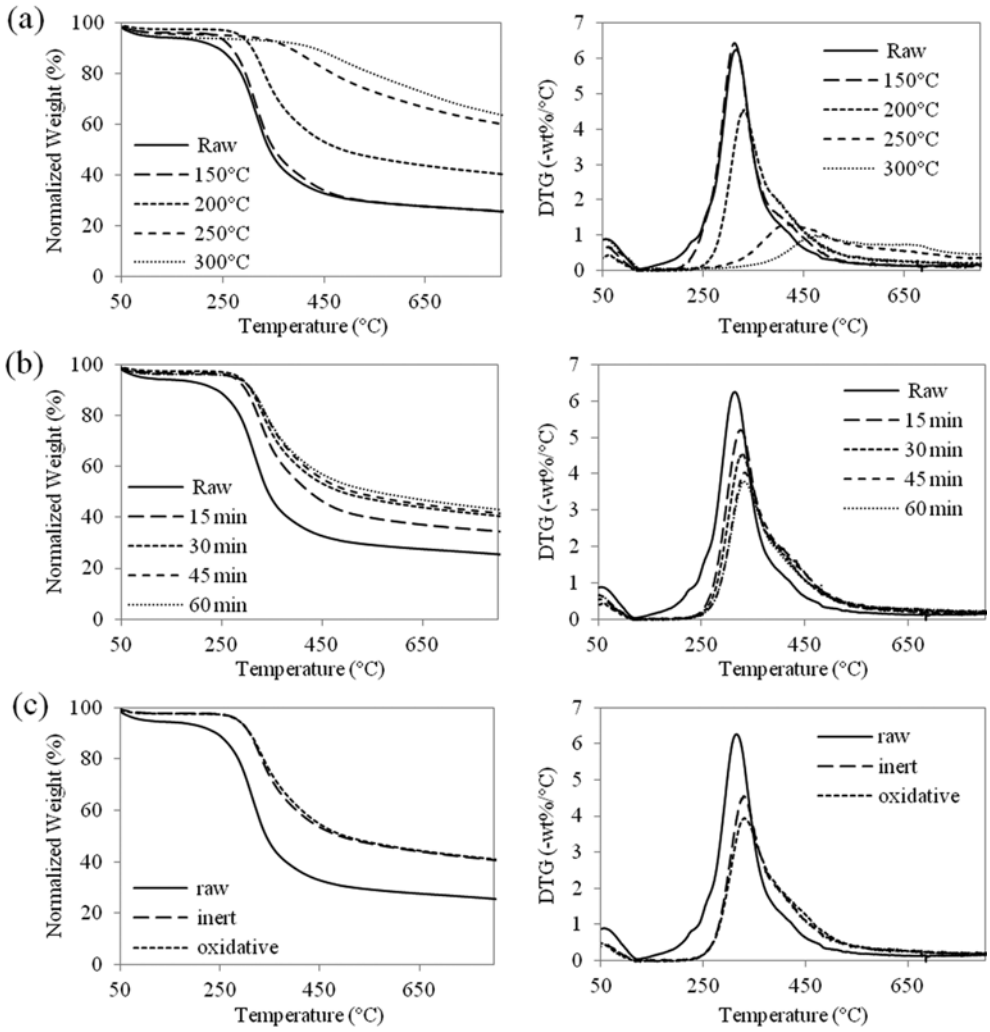

Fig. 6. Thermogravimetric (TGA) and Derivative Thermogravimetric (DTG) analysis of torrefied microalgae compared with raw material with (a) different torrefaction temperatures, (b) different torrefaction times, and (c) different atmospheres.

Table 3. Characteristics of devolatilization for raw and terrified microalgae

Samples	T_o (°C)	T_{max} (°C)	DTG_{max} (wt%/°C)	Residue (wt%)
Raw material	120	315	6.26	25.60
150 °C, 30 min	190	312	6.47	25.94
200 °C, 15 min	230	326	5.21	34.68
200 °C, 30 min	230	330	4.56	40.62
200 °C, 45 min	230	334	4.03	41.72
200 °C, 60 min	230	334	3.80	43.26
200 °C, 30 min, oxidative	230	331	3.95	41.08
250 °C, 30 min	250	416	1.31	60.36
300 °C, 30 min	280	474	1.02	63.79

are shown in Fig. 6, and the characteristic parameters of the devolatilization are summarized in Table 3. All curves show two clear weight loss regions, indicating the evaporation of moisture from the samples below 120 °C, and the main thermal decomposition above 120 °C. Under different torrefaction temperatures, times and atmospheres, it is apparent that the thermal decomposition behavior of the products was different from that of the raw material. The moisture evaluation peak in DTG curves of the torrefied samples is less pronounced because the hydroxyl group of the material was destroyed during the torrefaction process [20]. In addition, by torrefaction, some reactive fractions were released from the biomass. Therefore, the onset temperatures (T_o) and residual weight at 800 °C of the torrefied samples increased as the torrefaction temperature and time increased. When the torrefaction was carried out at 150 °C, the distribution of TGA and DTG was similar to that of raw microalgae. When the torrefaction temperature was increased to 200 °C, 250 °C, and 300 °C, the peaks of torrefied samples were more significantly different from those of the raw material, at 330 °C, 416 °C and 474 °C, respectively. The DTG curves of the torrefied samples at different torrefaction times were similar, featuring small T_{max} changes at higher temperatures with increased time. Similar result can be seen in the case of different atmospheres.

The main thermal degradation of the microalgae took place as a two-step process. First, the main degradation of proteins and par-

tial carbohydrates with a maximum DTG peak was around 312-334 °C. Second, the shoulder is formed in the DTG curves around 400-480 °C due to the decomposition of partial carbohydrates and lipids in microalgae. Torrefaction led to the loss of some proteins and carbohydrates; thus the shoulders of the DTG curves of the torrefied samples were more obvious. Furthermore, the degradation rate (DTG_{max}) of the main devolatilization for all the torrefied microalgae was lower than that of the raw material, but the degradation rate of the high temperature region, mainly assigned to decomposition of lipids, was higher. The torrefaction process probably accelerated this degradation by weakening the linkages of the chemical components.

CONCLUSIONS

The torrefaction of *Chlorella vulgaris* microalgae was studied across a range of torrefaction temperatures (150 °C to 300 °C), times (15 min to 60 min), and atmospheres (inert or oxidative). In the torrefaction of microalgae, the solid yield and the changes of biomass properties from the raw material were influenced more by the torrefaction temperature than by the time and atmosphere. The torrefied biomass yield decreased with increments of torrefaction temperature and time. The oxidative atmosphere also led to lower yields of torrefied biomass. The compact structure of the raw material became looser and was broken into smaller particles with more cavitations when the torrefaction temperature was increased. In addition, the results show that carbon content, ash content, and fixed carbon content of torrefied biomass increased with increased torrefaction temperature and time. The material torrefied at 200 °C, for 30 min, under an inert atmosphere showed the highest calorific value (19.48 MJ/kg). However, at higher torrefaction temperatures and times, the calorific value decreased. Among the studied temperatures, 200 °C was found to be good enough for torrefaction of the microalgae as long as the solid yield (>50%) and calorific value are the main concern. The oxygen content, hydrogen content, and volatile matter of the torrefied biomass decreased with increased torrefaction temperature and time. In addition, it could be concluded from the reactivity study that the decomposition of the protein and carbohydrate fractions in the torrefied biomass lowered the thermal degradation rate of these components, and that the thermal degradation rate of lipids was accelerated by torrefaction. Therefore, the torrefaction conditions influenced the changes in physical properties, chemical compositions and reactivity of torrefied microalgal biomass. This study may provide useful information for the development of industrial processes for the torrefaction of microalgae.

ACKNOWLEDGEMENT

The research was supported by a grant from Prince of Songkla University, contract no. SCI570531S. Also thanks to Mr.Thomas Coyne for assistance with the English.

REFERENCES

1. A. Uslu, A. P. C. Faaij and P. C. A. Bergman, *Energy*, **33**, 1206 (2008).
2. K.-M. Lu, W.-J. Lee, W.-H. Chen and T.-C. Lin, *Appl. Energy*, **105**, 57 (2013).
3. W.-H. Chen, J. Peng and X. T. Bi, *Renewable Sustainable Energy Rev.*, **44**, 847 (2015).
4. W.-H. Chen, K.-M. Lu, S.-H. Liu, C.-M. Tsai, W.-J. Lee and T.-C. Lin, *Bioresour. Technol.*, **146**, 152 (2013).
5. B. Batidzirai, A. P. R. Mignot, W. B. Schakel, H. M. Junginger and A. P. C. Faaij, *Energy*, **62**, 196 (2013).
6. C. Wang, J. Peng, H. Li, X. T. Bi, R. Legros, C. J. Lim and S. Sokhansanj, *Bioresour. Technol.*, **127**, 318 (2013).
7. K.-M. Lu, W.-J. Lee, W.-H. Chen, S.-H. Liu and T.-C. Lin, *Bioresour. Technol.*, **123**, 98 (2012).
8. B. Arias, C. Pevida, J. Fermoso, M. G. Plaza, F. Rubiera and J. J. Pis, *Fuel Process. Technol.*, **89**, 169 (2008).
9. B. Patel, B. Gami and H. Bhimani, *Energy Sustainable Dev.*, **15**, 372 (2011).
10. M. J. C. van der Stelt, H. Gerhauser, J. H. A. Kiel and K. J. Ptasinski, *Biomass Bioenergy*, **35**, 3748 (2011).
11. M. Phanphanich and S. Mani, *Bioresour. Technol.*, **102**, 1246 (2011).
12. T. G. Bridgeman, J. M. Jones, I. Shield and P. T. Williams, *Fuel*, **87**, 844 (2008).
13. A. Pimchuai, A. Dutta and P. Basu, *Energy Fuels*, **24**, 4638 (2010).
14. J. Li, A. Brzdekiewicz, W. Yang and W. Blasiak, *Appl. Energy*, **99**, 344 (2012).
15. M. Sarkar, A. Kumar, J. S. Tumuluru, K. N. Patil and D. D. Bellmer, *Appl. Energy*, **127**, 194 (2014).
16. L. Cao, X. Yuan, H. Li, C. Li, Z. Xiao, L. Jiang, B. Huang, Z. Xiao, X. Chen, H. Wang and G. Zeng, *Bioresour. Technol.*, **185**, 254 (2015).
17. B. Ru, S. Wang, G. Dai and L. Zhang, *Energy Fuels*, **29**, 5865 (2015).
18. J. Poudel, T.-I. Ohm and S. C. Oh, *Fuel*, **140**, 275 (2015).
19. M. Atienza-Martínez, J. F. Mastral, J. Ábrego, J. Ceamanos and G. Gea, *Energy Fuels*, **29**, 160 (2015).
20. K.-T. Wu, C.-J. Tsai, C.-S. Chen and H.-W. Chen, *Appl. Energy*, **100**, 52 (2012).
21. Y. Uemura, R. Matsumoto, S. Saadon and Y. Matsumura, *Fuel Process. Technol.*, **138**, 133 (2015).
22. W.-H. Chen and P.-C. Kuo, *Energy*, **35**, 2580 (2010).
23. W.-H. Chen and P.-C. Kuo, *Energy*, **36**, 803 (2011).
24. M. J. Prins, K. J. Ptasinski and F. J. J. G. Janssen, *J. Anal. Appl. Pyrolysis*, **77**, 35 (2006).
25. A. Dhungana, P. Basu and A. Dutta, *J. Energy Resour. Technol.*, **134**, 041801 (2012).
26. D. Tapasvi, R. Khalil, ∅. Skreiberg, K.-Q. Tran and M. Grnli, *Energy Fuels*, **26**, 5232 (2012).
27. W.-H. Chen, Y.-Q. Zhuang, S.-H. Liu, T.-T. Juang and C.-M. Tsai, *Bioresour. Technol.*, **199**, 367 (2016).
28. N. R. Moheimani, M. A. Borowitzka, A. Isdepsky and S. F. Sing, in *Algae for Biofuels and Energy*, M. A. Borowitzka and N. R. Moheimani Eds., Springer, Netherlands (2013).
29. M. Mecozzi, *Chemom. Intell. Lab. Syst.*, **79**, 84 (2005).
30. F. Smedes and T. K. Thomasen, *Mar. Pollut. Bull.*, **32**, 681 (1996).
31. A. Friedl, E. Padouvas, H. Rotter and K. Varmuza, *Anal. Chim. Acta*, **544**, 191 (2005).
32. J. Deng, G.-J. Wang, J.-H. Kuang, Y.-L. Zhang and Y.-H. Luo, *J.*

Anal. Appl. Pyrolysis, **86**, 331 (2009).
33. W.-H. Chen, H.-C. Hsu, K.-M. Lu, W.-J. Lee and T.-C. Lin, *Energy*, **36**, 3012 (2011).
34. Y. Uemura, W. Omar, N. A. Othman, S. Yusup and T. Tsutsui, *Fuel*, **103**, 156 (2013).
35. Y.-C. Chen, W.-H. Chen, B.-J. Lin, J.-S. Chang and H. C. Ong, *Appl. Energy*, **181**, 110 (2016).
36. M. M. Phukan, R. S. Chutia, B. K. Konwar and R. Kataki, *Appl. Energy*, **88**, 3307 (2011).
37. R. H. H. Ibrahim, L. I. Darvell, J. M. Jones and A. Williams, *J. Anal. Appl. Pyrolysis*, **103**, 21 (2013).
38. K. Stehfest, J. Toepel and C. Wilhelm, *Plant Physiol. Biochem.*, **43**, 717 (2005).
39. M. Mecozzi, M. Pietroletti and A. Tornambè, *Spectrochim. Acta, Part A*, **78**, 1572 (2011).